

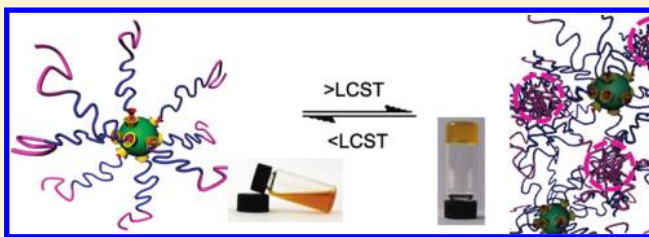
Dual Responsive Supramolecular Hydrogel with Electrochemical Activity

Ping Du, Jianghua Liu, Guosong Chen,* and Ming Jiang*

Key Laboratory of Molecular Engineering of Polymers, Ministry of Education, and Department of Macromolecular Science, Fudan University, Shanghai 200433, People's Republic of China

Supporting Information

ABSTRACT: Supramolecular materials with reversible responsiveness to environmental changes are of particular research interest in recent years. Inclusion complexation between cyclodextrin (CD) and ferrocene (Fc) is well-known and extensively studied because of its reversible association–dissociation controlled by the redox state of Fc. Although there are quite a few reported nanoscale materials incorporating this host–guest pair, polymeric hydrogels with electrochemical activity based on this interactive pair are still rare. Taking advantage of our previous reported hybrid inclusion complex (HIC) hydrogel structure, a new Fc–HIC was designed and obtained with β -CD-modified quantum dots as the core and Fc-ended diblock co-polymer p(DMA-*b*-NIPAM) as the shell, to achieve an electrochemically active hydrogel at elevated temperatures. Considering the two independent cross-linking strategies in the network structure, i.e., the interchain aggregation of pNIPAM and inclusion complexation between CD and Fc on the surface of the quantum dots, the hydrogel was fully thermo-reversible and its gel–sol transition was achieved after the addition of either an oxidizing agent or a competitive guest to Fc.



INTRODUCTION

Supramolecular materials with reversible responsiveness to environmental changes are of particular research interest in recent years. The achievement of supramolecular chemistry greatly promotes the development of ferrocene (Fc)-associated electrochemical responsive materials, because Fc can form inclusion complexes with macrocyclic molecules,^{1–3} e.g., cyclodextrins (CDs).^{4–8} The most important fact is that Fc in its reduced state, as a neutral compound, binds to CDs, while its oxidized state ferrocenium (Fc⁺), as a cation, binds very weakly.⁴ This has brought much free space for polymer scientists to develop responsive materials controlled by this electrochemical reversible complex. Many electrochemical responsive supramolecular systems⁹ have been achieved, but most of them were the self-assemblies on surface^{10–13} or in diluted solutions,^{14,15} including micelles or vesicles.^{16,17} Up to now, polymeric hydrogel with electrochemical activity based on this inclusion complexation is very limited. As far as we know, only one redox responsive hydrogel has been reported,¹⁸ in which Fc was added as a competitive guest to dissociate the existed inclusion complexation between the alkyl chain and CD in hydrogel.

Our group has focused on responsive polymeric hydrogels with CD-based inclusion complexation as the “supramolecular crosslinking” strategy.¹⁹ Very recently, we demonstrated that, inorganic nanoparticles covered by CD cavities, so-called supracrosslink,²⁰ could construct polymeric networks via inclusion complexation with suitable guest molecules on polymers. This strategy has been proven very efficient to achieve sol–gel

transition by supramolecular means, without using high-molecular-weight polymeric networks or triblock co-polymers,²¹ and thus inspired us to explore electrochemically active hydrogel with polymers containing Fc moieties. Herein, we report the first polymeric hydrogel based on the inclusion complexation between CD and Fc with electrochemical activity and dual responsiveness.

RESULTS AND DISCUSSION

Design of Fc–HIC and Synthesis of Fc-Ended Block Copolymer. Our previously reported hybrid inclusion complex (HIC)²¹ structure has been further employed to construct this novel electrochemically active hydrogel. The building blocks in this work include β -CD-modified CdS quantum dot (CD@QD) and block co-polymer poly(*N,N'*-dimethylacrylamide)-*b*-poly(*N*-isopropylacrylamide) with a Fc-functionalized end [Fc–p(DMA-*b*-NIPAM)], as shown in Figure 1. Because of the inclusion complexation between CD and Fc, this multi-arm superstructure, which is named Fc–HIC, would form with a QD core and block co-polymer arms, where the pNIPAM block is in the outer layer at room temperature. After temperature increases above the lower critical solution temperature (LCST) of pNIPAM, the pNIPAM block may aggregate to form

Received: May 17, 2011

Revised: June 21, 2011

Published: June 23, 2011

microdomains, which serve as another cross-link factor besides the QD core, and bring the initial Fc–HIC to hydrogel.

To obtain our desired block co-polymer Fc–p(DMA-*b*-NIPAM) with Fc end functionality, we used reversible addition–fragmentation chain-transfer (RAFT) polymerization because of its versatile and well-controllable characters. Recently, the RAFT polymerization started from Fc was studied by Zhu et al.²² In the present work, a new Fc-modified chain-transfer agent (Fc–CTA) was designed and prepared as shown in Scheme 1. The synthesis started from the commercially available ferrocenecarboxylic acid (FcCOOH). After two-step conventional esterification reactions, a novel Fc–CTA was obtained with a reasonable yield (Scheme 1). The RAFT polymerization of the first block pDMA was stopped at about 80% monomer consumption to ensure the existence of trithiocarbonate on the polymer chain. Then, subsequently, the resulting homopolymer

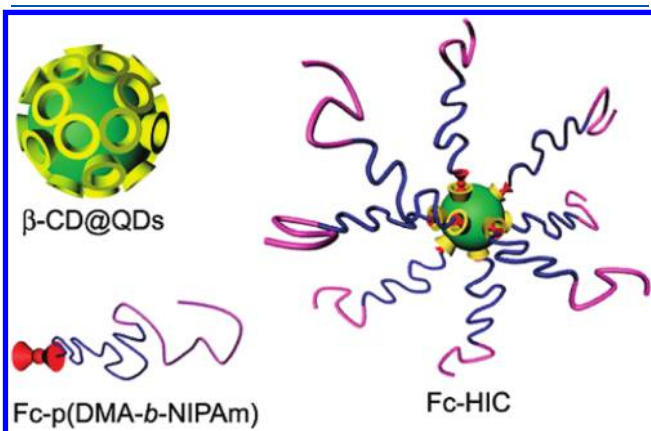
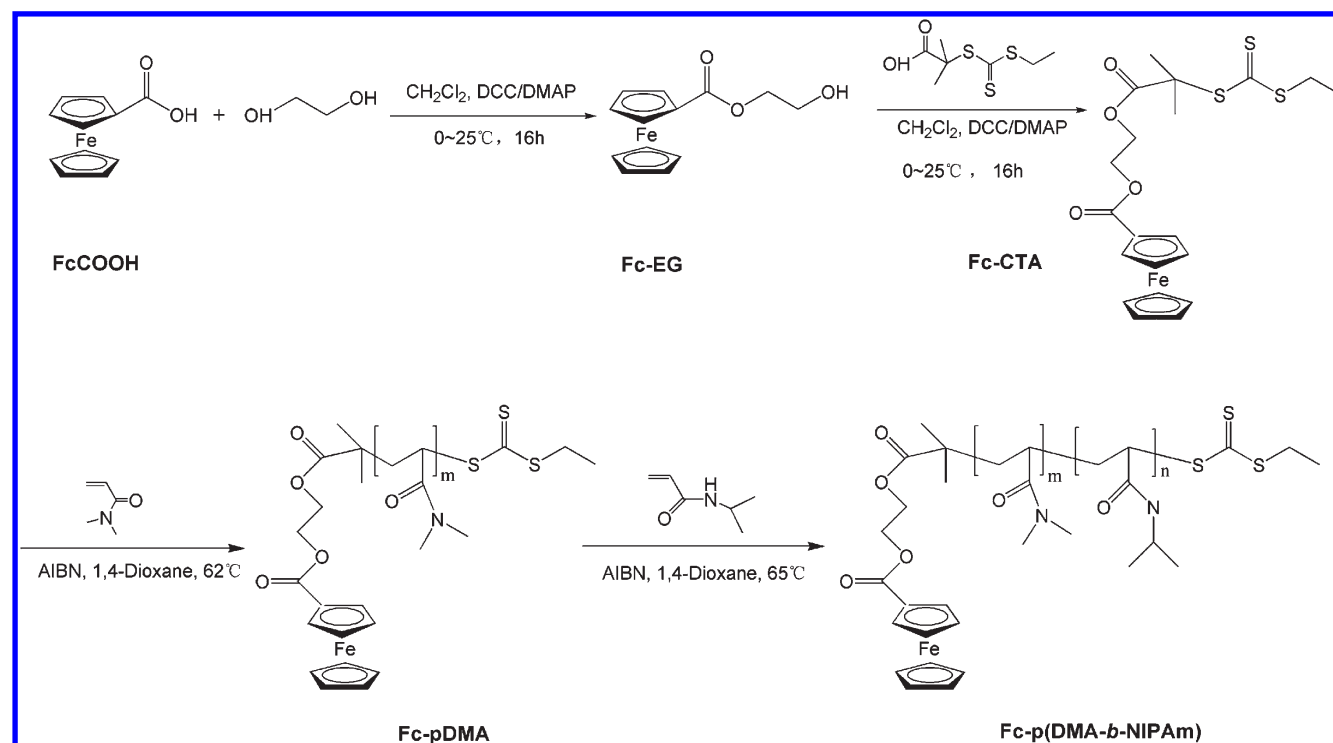


Figure 1. Illustration of block co-polymer Fc–p(DMA-*b*-NIPAM) and the corresponding Fc–HIC.

Fc–pDMA₉₅ [polydispersity index (PDI) of 1.13, obtained from gel permeation chromatography (GPC)] was further used as macro-Fc–CTA for the polymerization of NIPAM to yield the desired co-polymer as Fc–p(DMA₉₅-*b*-NIPAM₁₃₇) [Scheme 1; PDI of 1.21; M_w calculated from ¹H nuclear magnetic resonance (NMR)]. As seen from the GPC traces (Figure 2), a well-defined block co-polymer with a narrow molecular-weight distribution was successfully synthesized. It was interesting to find micellization of this co-polymer in water because of the hydrophobic interaction between Fc moieties. The critical micelle concentration (cmc) was found to be 4 mg/mL at room temperature as measured with pyrene as a fluorescent probe (Figure S5 in the Supporting Information). Considering the fully hydrophilicity of both pDMA and pNIPAM blocks in this condition, the micelle has Fc as the core and p(DMA-*b*-NIPAM) as the shell.

Formation of Fc–HIC and Its Electrochemical Property. With the desired Fc–p(DMA-*b*-NIPAM) in hand, we further prepared Fc–HIC with CD@QD as the core and the co-polymer as the shell, following our previous reported method.²¹ The QDs and co-polymers (mole ratio of host/guest = 2:1) were mixed in aqueous solution followed by sonication. Then, the uncomplexed components were removed by dialysis ($5 \times 10^4 M_w$ cut off). The success of inclusion complexation to form Fc–HIC was proven by Thermogravimetric analysis (TGA), showing 82.1% organic content in the complex compared to 48% of that in CD@QD (Figure S6 in the Supporting Information). This indicated that there was about 8 polymer chains and 22 CDs on 1 QD core. Furthermore, the formation of Fc–HIC was also demonstrated by photoluminescence spectra. The superstructure inherited the initial trap-state emissions of QDs, presenting a strong emission around 548 nm (Figure S7 in the Supporting Information). Although there are many reports about cyclic voltammetric (CV) behavior of Fc and its corresponding inclusion complex, measurements of the electrochemical property of

Scheme 1. Synthetic Route of the Fc–p(DMA-*b*-NIPAM) Block Co-polymer



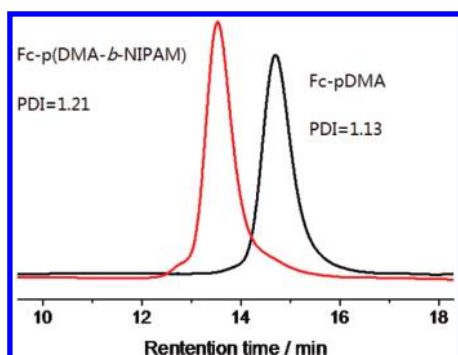


Figure 2. Molecular-weight distribution of macro-Fc-CTA (Fc-pDMA) and the corresponding diblock co-polymer Fc-p(DMA-*b*-NIPAM) obtained from GPC.

Fc on polymers, especially at the end of the polymer chain, is quite limited, because the Fc concentration is relatively low. Figure 3 shows the CV data of Fc-p(DMA-*b*-NIPAM) in the absence and presence of CD@QD. Clearly, after the addition of CD@QD, the peak retains its reversible shape but the half-wave potential ($E_{1/2}$) has been shifted to a more positive position. This anodic potential shift reveals that the Fc molecule is considerably more stabilized by inclusion complexation of CD than its oxidized form Fc^+ , which normally does not bind.³ This result fully supports the inclusion complexation between CD on the QD core and Fc from the co-polymer, confirming the formation of Fc-HIC. As reported in the literature,³ the inclusion complexation between Fc and CD not only induces an anodic shift of the corresponding $E_{1/2}$ but also a current level decrease, as a result of the restricted diffusion of Fc caused by the host-guest association. In our case, interestingly, an increase of the current level has been observed, which is contrary to this prevailing phenomenon. Obviously, the amphiphilicity of the current co-polymer here brings much more complexity to depict the Fc-associated electrochemical behavior than small molecular surfactants. For the case without CD@QD, the concentration of Fc-p(DMA-*b*-NIPAM) for the electrochemical measurement (30 mg/mL) is much higher than its cmc, which means that the hydrophobic Fc moieties are bonded together in the micelle core. Thus, the diffusion of Fc in Fc-HIC is possibly even less restricted than that when Fc is in the micellar core, leading to a higher current.

Formation of Supramolecular Hydrogel and Its Electrochemical Property. The Fc-HIC superstructure with the QD core and the co-polymer shell is ready to form hydrogel. In this Fc-HIC, there are two polymer layers, i.e., the inner one of pDMA, which is always kept solvated in water, and the outer one of pNIPAM, which turns to insoluble when the temperature is increased to above its LCST (data in Figure S8 in the Supporting Information). Thus, when the temperature is high enough, pNIPAM collapsed and combined with each other to form domains of the interchain aggregates, leading to network, i.e., hydrogel, formation (Figure 4). Normally, the electrochemical property is controlled by the diffusion rate of the active compound (Figure S9 in the Supporting Information). Therefore, it is usually hard to detect the electrochemical behavior when the active compound is confined in the bulk gel, because its diffusion rate is usually very low. Fortunately, because of the high cross-linking efficiency of the HIC structure to form hydrogel, which has been addressed in our previous study,²¹ the present hydrogel

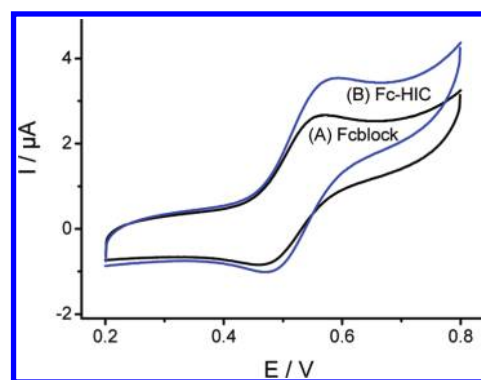


Figure 3. CV response on a glassy carbon electrode (0.25 cm^2) of a $1.2 \times 10^{-6} \text{ mM}$ Fc-p(DMA-*b*-NIPAM) aqueous solution with 0.1 M phosphate-buffered saline (PBS) as the supporting electrolyte in the (A) absence and (B) presence of CD@QD, with CD/Fc = 2:1 (molar ratio). The supporting electrolyte is 0.1 M PBS buffer solution (pH 7.2), and the scan rate is 50 mV/s.

can be achieved with a relatively low solid content (12.5 wt %). Thus, it provided an opportunity to observe the electrochemical property. In this experiment, a 20 wt % Fc-HIC solution was diluted to 12.5 wt % with 0.1 M PBS buffer as the supporting electrolyte and then preheated to 42 °C, which was above the LCST. Meanwhile, the electrolytic cell and the three electrodes were all preheated to 42 °C. Then, a thin layer of hydrogel was quickly coated on the surface of the working electrode. As shown in Figure 4, the fully reversible electrochemical behavior of the Fc-HIC hydrogel on the electrode has been recorded. This experiment clearly proves the electrochemical activity of the hybrid hydrogel. As far as we know, this is the first reported electrochemical cycle of polymeric hydrogel containing Fc moieties.

Steady and Dynamic Rheology Study of the Fc-HIC Hydrogel. Figure 5 showed viscosity variation of the co-polymer Fc-p(DMA-*b*-NIPAM) and Fc-HIC, when the temperature was increased from 25 to 50 °C, at a rate of 1 °C/min. The solid content of both samples was set as 12.5 wt %. As shown in Figure 5, in the testing temperature range from 25 to 50 °C, viscosity of the co-polymer solution changed little (line B), while the solution of Fc-HIC showed an abrupt viscosity enhancement from 35 to 43 °C (line A) above the LCST of pNIPAM. The maximum viscosity reached about 55 Pa s, about 100 times higher than that of the co-polymer, proving the cross-linking efficiency of the CD@QD core in the Fc-HIC structure. With a further temperature increase, hydration of the pNIPAM segment took place and part of the water was released, resulting in a little decrease of the viscosity.

Dynamic rheology was employed to monitor the *in situ* sol-gel transition of the Fc-HIC solution and then to measure the gelation point, where the storage (or elastic) modulus G' curve surpasses that of the loss (or viscous) modulus G'' . Figure 6 shows the oscillatory temperature sweep profiles of Fc-HIC at a constant shear frequency (1 Hz) at a concentration of 12.5 wt %. Below 33 °C, the Fc-HIC aqueous solutions exhibited obvious viscoelastic response, where G'' was larger than G' , indicating that the Fc-HIC was in a liquid state. In this temperature range, both G' and G'' varied little with the temperature increase. When the temperature was increased above 33 °C, pNIPAM began to dehydrate and aggregate. The Fc-HIC solution turned into a "gel-like" state because of the formation of the cross-linked

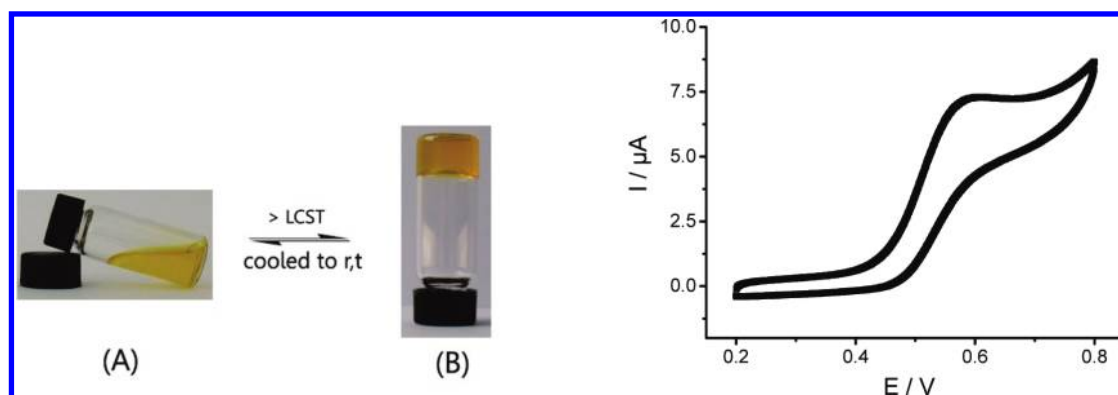


Figure 4. Image of the (left) thermal Fc-HIC sol-gel transition and (right) electrochemical property of the hydrogel.

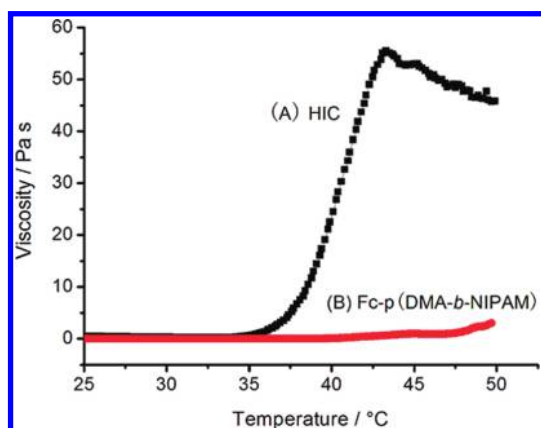


Figure 5. Steady-state rheology measurement of (A) Fc-HIC and (B) co-polymer Fc-p(DMA-*b*-NIPAM).

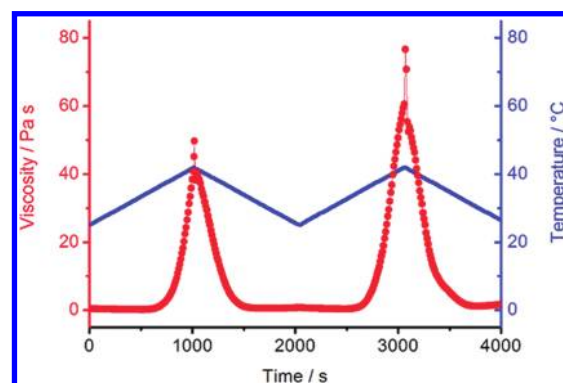


Figure 7. Viscosity variations of Fc-HIC solution (12.5 wt %) during heating-cooling cycles.

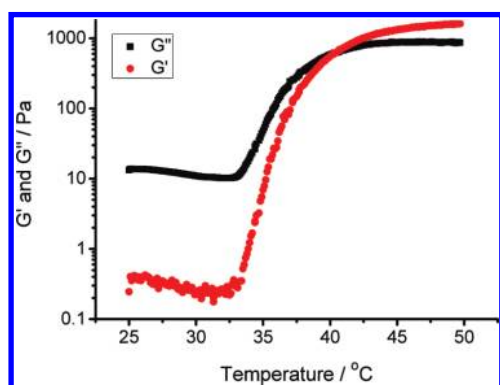


Figure 6. Dynamic rheology study of the Fc-HIC hydrogel.

network. At this temperature range, both G' and G'' increased. However, the enhancement rate of G' was larger than that of G'' because the elastic properties started to dominate. The crossover point of G' and G'' was at 40.5 °C, indicating that a sol-gel transition occurred.

Thermal and Redox Responsiveness of the Fc-HIC Hydrogel. Because the Fc-HIC supramolecular hydrogel was induced by both a temperature increase and host-guest inclusion complexation, its sol-gel transition can be observed by changing either of the factors. The viscosity changes versus the temperature cycles had been demonstrated in Figure 7. When the temperature reached 33 °C, the Fc-HIC supramolecular

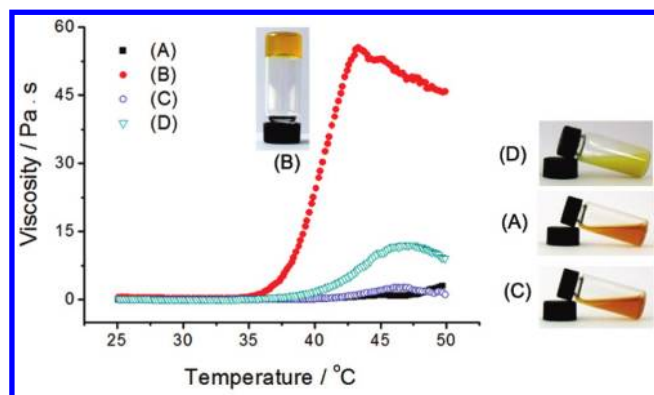
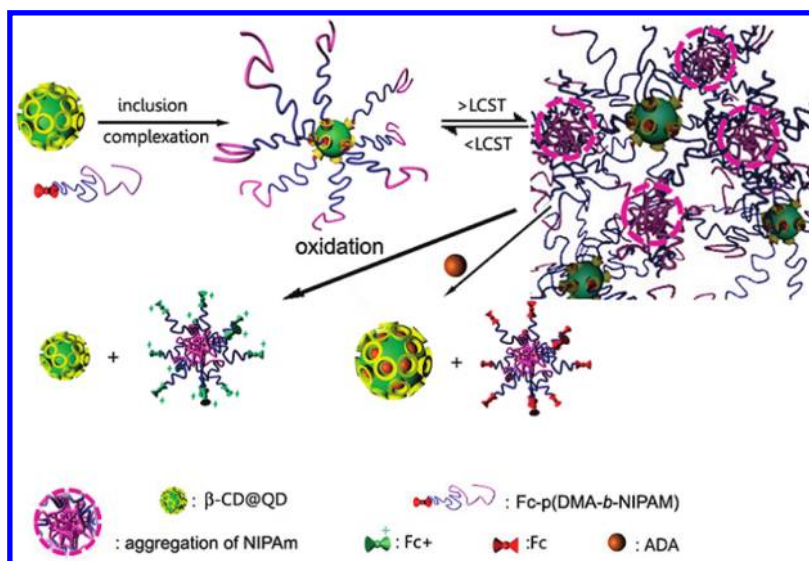


Figure 8. Steady-state rheology measurements and photos of (A) copolymer Fc-p(DMA-*b*-NIPAM), (B) Fc-HIC supramolecular hydrogel, (C) ADA-dissociated Fc-HIC hydrogel, and (D) sol of the hydrogel after $K_3Fe(CN)_6$ oxidation.

hydrogel began to form, as indicated by the abrupt viscosity increase. When the hydrogel was then cooled to room temperature, the aggregated pNIPAM became hydrated again, resulting in the dissociation of the thermal responsive network. At this moment, the free-standing gel flowed again as a liquid. As shown in Figure 7, with a linear increase of the temperature, the viscosity of Fc-HIC increased from 0.4 Pa s at 25 °C to 45.2 Pa s at 42 °C and then decreased to the original 0.5 Pa s, when the temperature was decreased to 25 °C, showing a perfect reversibility. In the

Scheme 2. Schematic Illustration of the Formation and Dissociation of the Supramolecular Fc–HIC Hydrogel



second cycle, because of evaporation of a small amount of water, the maximum viscosity of the hydrogel was a little higher than that in the first cycle.

As discussed before, the inclusion complexation between Fc and CD serves as another cross-linker in this Fc–HIC hydrogel. Thus, dissociation of the inclusion complex may also lead to the gel–sol transition. Generally, there are two ways to achieve this goal. One is to oxidize Fc into Fc^+ , because the latter binds to CD very weakly. $\text{K}_3\text{Fe}(\text{CN})_6$ was chosen as the oxidization agent.²³ After the addition of 3 mg of $\text{K}_3\text{Fe}(\text{CN})_6$ to the Fc–HIC hydrogel, as shown in Figure 8D, the gel–sol transition took place within 30 min. The other one is adding a competitive host or guest, which binds stronger than and then dissociates the original guest/host complex. Because β -CD gives a higher binding ability to Fc than α -CD and γ -CD,²⁴ adding a competitive host molecule is not practical. Then, sodium 1-adamantanecarboxylate (ADA) as the competitive guest was employed. ADA was proven efficient to dissociate the Fc–HIC cross-link and induce the gel–sol transition (Figure 8C) in less than 10 min. Meanwhile, the rheology study proved that the resultant solution obtained from both chemical oxidation and supramolecular competition showed much lower viscosity than Fc–HIC measured above the LCST (Figure 8 and dynamic data in Figure S10 in the Supporting Information). The success in this supramolecular strategy to realize the gel–sol transition (Scheme 2), which is similar to that used in our previous systems, proved to be a great advantage of our supramolecular hydrogels, i.e., fast and convenient gel–sol responsiveness.

CONCLUSION

We successfully achieved polymeric hydrogels with an electrochemical activity from the so-called Fc–HIC structure, with CD covered QD as the core and Fc-ended co-polymer Fc–p(DMA-*b*-NIPAM) as the shell. The obtained hydrogel above the LCST of pNIPAM showed satisfactory temperature-reversible sol–gel transitions as well as the responsiveness to chemical oxidation and supramolecular competition.

EXPERIMENTAL SECTION

Materials. *N,N*-Dimethylacrylamide (DMA, distilled under reduced pressure before polymerization) and *N*-isopropylacrylamide [NIPAM, recrystallized 3 times from benzene/hexane (6:4, v/v) prior to use] were purchased from TCI. Azodiisobutyronitrile (AIBN, CP, recrystallized from ethanol before use) and β -cyclodextrin (β -CD, CP, recrystallized twice from deionized water) were supplied by Sinopharm Chemical Reagent Co. Modified CdS quantum dots (β -CD@QD) was prepared as our previously reported method.²¹ Ferrocenecarboxylic acid (FcCOOH , 98+%, recrystallized twice from dichloromethane/petroleum ether) was purchased from the Yixing Weite Petrochemical Additives Plant, and ADA was prepared from adamantanecarboxylic acid (purchased from Alfa Aesar), with equivalent amounts of sodium hydroxide. Unless specially mentioned, all other chemicals were used as received.

Measurements. ^1H NMR spectra were recorded with a Bruker 400 MHz NMR spectrometer. Samples were prepared in CDCl_3 . GPC analysis was carried out with a Waters Breeze 1525 GPC analysis system with two PL mix-D columns, using *N,N*-dimethylformamide (DMF) with 0.5 M LiBr as eluents at the flow rate of 1 mL/min at 80 °C with a poly(ethylene oxide) (PEO) calibration kit (purchased from TOSOH) as the calibration standard. Ultraviolet–visible (UV–vis) spectra were recorded in a conventional quartz cell (light path of 10 mm) on a Perkin-Elmer Lambda 35 spectrophotometer. TGA measurements were carried out on a Perkin-Elmer Pyris-1 series thermal analysis system under a flowing nitrogen atmosphere at a scan rate of 20 °C min^{-1} from 100 to 550 °C. Electrospray ionization–mass spectrometry (ESI–MS) analyses were performed with an Applied Biosystems API 95 (San Jose, CA) model LCQ ion-trap mass spectrometer equipped with an ESI source and Analyst software. The fluorescence spectra of β -CD@QD and Fc–HIC were measured by FL920 (Edinburg Instruments), equipped with a photomultiplier tube (excitation wavelength of 365 nm). For the cmc measurement, pyrene was used as a fluorescence probe at a concentration of 6.0×10^{-4} mg/mL using an excitation wavelength of 339 nm. The intensity ratio of the first to third peak (I_1/I_3) of the pyrene emission spectrum was plotted as a function of the block co-polymer concentration. The rheological behavior of the samples was measured by Bohlin GeminiHRnano Rheology equipment, fitted with a parallel plate (diameter of 40 mm) and circulating environmental system for temperature control. The sample chamber was sealed by water. The gap

distance between the two parallel plates was fixed at 0.2 mm. The gel formation process was investigated by increasing the temperature at a rate of 1 °C/min. The study of the thermoreversibility of the samples (Figure 7) was performed by an increase and a decrease of the temperature at a rate of 1 °C/min. Steady rheology measurements were performed by a steady-step temperature-ramp test (strain-controlled) at the same shear rate (1 s⁻¹). Dynamic rheology measurements were performed by oscillatory temperature sweeps (stress-controlled) at the oscillation frequency of 1.0 Hz and the deformation of 0.1%.

Electrochemical Measurements. CV was recorded in a three-electrode cell using a model CHI650 electrochemical workstation at 20 °C. A glass carbon electrode (GCE) (5 mm diameter) was used as the working electrode with a platinum plate (Pt) as the counter electrode and a saturated calomel electrode (SCE) as the reference electrode. Prior to each experiment, the glassy carbon electrode was first polished with α -alumina powder, rinsed thoroughly with triply distilled water, then sonicated successively in a 1:1 mixture of nitric acid and water, and finally, washed by triply distilled water. PBS (pH 7.2) solution of 0.1 M was used as a supporting electrolyte to dissolve the samples, and the final solid content was set as 30 mg/mL. The potential was scanned from 0.2 to 0.8 V versus SCE, at a scan rate of 50 mV/s.

Preparation of Fc-CTA. Fc-EG was first synthesized by a conventional *N,N'*-dicyclohexylcarbodiimide (DCC)-mediated esterification of FcCOOH with ethylene glycol. The synthesis process is as follows: FcCOOH (4.60 g, 20 mmol) and 4-dimethylaminopyridine (DMAP, 2.44 g, 20 mmol) were dissolved in 100 mL of dichloromethane (DCM), and then ethylene glycol (EG, 2.48 g, 40 mmol) in 10 mL of DCM and DCC (6.19 g, 30 mmol) in 20 mL of DCM were added. The resulting mixture was stirred at room temperature for 16 h. Then, the precipitate was removed by filtration. The filtrate was concentrated under reduced pressure and purified on a 200–300 mesh silica gel column with an elution solvent of hexane/ethyl acetate (4:1, v/v), affording 3.4 g (yield 67%) of the product. ¹H NMR (Figure S1 in the Supporting Information) (400 MHz, CDCl₃) δ : 4.83 (*t*, *J* = 1.9 Hz, 2H, Fc), 4.42 (*t*, *J* = 1.9 Hz, 2H, Fc), 4.38 (*t*, *J* = 4.6 Hz, 2H, CH₂CH₂OH), 3.92 (*t*, *J* = 4.6 Hz, 2H, CH₂CH₂OH), 4.22 (*s*, 5H, Fc), 2.18 (*s*, OH). ESI-MS: 275.4 [M + H]⁺, 297.3 [M + Na]⁺. Calcd 274.09 (C₁₃H₁₄O₃Fe).

Trithiocarbonate acid (*S*-ethyl-*S'*-(α,α' -dimethyl- α'' -acetic acid)-trithiocarbonate) was prepared as a previously reported method.²⁵ Fc-CTA was synthesized by another DCC-mediated condensation started from Fc-EG with trithiocarbonate acid. Trithiocarbonate acid (3.60 g, 0.016 mol), Fc-EG (3.3 g, 0.012 mol), and DMAP (0.73 g, 0.006 mol) were dissolved in dry DCM (30 mL) in an ice bath, and then DCC (4.95 g, 0.024 mol) in 10 mL of DCM was added dropwise. After the reaction was carried out at room temperature for 16 h, the resultant mixture was filtered to remove the white precipitate. Then, the filtrate was washed twice with water and dried over sodium sulfate. The crude product was purified by a silica gel column, eluted by hexane/ethyl acetate (15:1, v/v). ¹H NMR (Figure S2 in the Supporting Information) (400 MHz, CDCl₃) δ : 4.79 (*s*, 2H, Fc), 4.39 (*s*, 2H, Fc; 4H, OCH₂CH₂O), 4.20 (*s*, 5H, Fc), 3.22–3.28 (*q*, *J* = 7.2 Hz, 2H, CH₂CH₃), 1.72 (*s*, 6H, C(CH₃)₂), 1.28–1.32 (*t*, *J* = 7.2 Hz, 3H, CH₂-CH₃). ESI-MS: 481.4 [M + H]⁺, 498.3 [M + NH₄]⁺. Calcd 480.44 (C₂₀H₂₄O₄S₃Fe).

RAFT Polymerization of Fc-pDMA (Macro-Fc-CTA). Fc-CTA (0.480 g, 1.0 mmol), AIBN (0.0116 g, 0.1 mmol), DMA (13.88 g, 140 mmol), and 30 mL of 1,4-dioxane were added into a 75 mL flask equipped with a magnetic stirring bar. After the mixed solution was degassed by freeze–pump–thaw cycles for 3 times, it was transferred to an oil bath, which had been preheated to 62 °C, to initiate the polymerization. The polymerization was carried out for 2.5 h and then quenched by liquid nitrogen. The resulting mixture was precipitated in cooled diethyl ether to obtain the crude product, which was

subsequently dissolved in THF and then precipitated in diethyl ether for 3 times to remove unreacted monomers. The final product was dried *in vacuo*, yielding a yellow solid (10.2 g, 72%, $M_{n,GPC} = 5.12 \times 10^3$, $M_w,GPC/M_{n,GPC} = 1.13$). The degree of polymerization of the obtained polymer was 95, which was determined by the integrals of signals corresponding to Fc at δ 4.20–4.80 and DMA block at δ 2.76–3.04 according to ¹H NMR (Figure S3 in the Supporting Information).

RAFT Polymerization of Block Co-polymer Fc-p(DMA-*b*-NIPAM). Starting from the previous obtained macro-Fc-CTA, the polymerization was carried out with a [NIPAM]/[macro-Fc-CTA]/[AIBN] ratio as 180:1:0.2. A solution of NIPAM (8.14 g, 72 mmol), macro-Fc-CTA (4.0 g, 4×10^{-4} mol), and AIBN (9.30 mg, 8.0×10^{-4} mol) in 24 mL of 1,4-dioxane in a 75 mL flask, equipped with a magnetic stirring bar, was degassed by freeze–pump–thaw cycles for 3 times. Then, the flask was immediately immersed in an oil bath preheated at 70 °C. After stirring for 3.5 h, the polymerization was terminated by liquid N₂ and the resultant mixture was precipitated into an excess diethyl ether. The crude product was redissolved in THF and precipitated in excess diethyl ether for 3 times to remove the unreacted NIPAM monomer, yielding the desired co-polymer (9.47 g, 78%, $M_{n,GPC} = 1.45 \times 10^4$, $M_w,GPC/M_{n,GPC} = 1.21$). The degree of polymerization of the PNIPAM block of Fc-p(DMA-*b*-NIPAM) was 137, which was determined on the basis of the integrals of the signals corresponding to DMA at δ 2.76–3.04 and NIPAM at δ 4.00 according to ¹H NMR (Figure S4 in the Supporting Information).

Preparation of the Supramolecular Hydrogel. A total of 34 mg of β -CD@QD was taken into a 5 mL glass vial containing 0.80 mL of water. After β -CD@QD was dissolved completely in a few minutes, 166 mg of co-polymer Fc-p(DMA-*b*-NIPAM) was added to the yellow solution. Here, the molar ratio of β -CD in β -CD@QD and the Fc units in the co-polymer is around 2:1. Then, the mixture was diluted with 0.60 mL of water to reach the final solid content of 12.5 wt %. The mixture was stirred to ensure the inclusion complexation. Hydrogel formed directly after heating the mixture at 42 °C for 0.5 h.

■ ASSOCIATED CONTENT

Supporting Information. Characterizations of block copolymers and hydrogels (Figures S1–S9). This material is available free of charge via the Internet at <http://pubs.acs.org>.

■ AUTHOR INFORMATION

Corresponding Author

*E-mail: guosong@fudan.edu.cn (G.C.); mjiang@fudan.edu.cn (M.J.).

■ ACKNOWLEDGMENT

The National Natural Science Foundation of China (20834004 and 20904005) and the Ministry of Science and Technology of China (2009CB930402 and 2011CB932503) are acknowledged for their financial support.

■ REFERENCES

- (1) Podkoscilny, D.; Hooley, R. J.; Rebek, J.; Kaifer, A. E. *Org. Lett.* **2008**, *10*, 2865–2868.
- (2) Liu, J.; Alvarez, J.; Ong, W.; Román, E.; Kaifer, A. E. *Langmuir* **2001**, *17*, 6762–6764.
- (3) Kaifer, A. E. *Acc. Chem. Res.* **1999**, *32*, 62–71.
- (4) Matsue, T.; Evans, D. H.; Osa, T.; Kobayashi, N. *J. Am. Chem. Soc.* **1985**, *107*, 3411–3417.

- (5) Casas-Solvas, J. M.; Ortiz-Salmerón, E.; Fernández, I.; García-Fuentes, L.; Santoyo-González, F.; Vargas-Berenguel, A. *Chem.—Eur. J.* **2009**, *15*, 8146–8162.
- (6) Liu, Y.; Cao, R.; Chen, Y.; He, J. Y. *J. Phys. Chem. B* **2008**, *112*, 1445–1450.
- (7) Han, Y. B.; Cheng, K. J.; Simon, K. A.; Lan, Y. M.; Sejwal, P.; Luk, Y. Y. *J. Am. Chem. Soc.* **2006**, *128*, 13913–13920.
- (8) Fernandes, J. A.; Lima, S.; Braga, S. S.; Pillinger, M.; Ribeiro-Claro, P.; Rodriguez-Borges, J. E.; Lopes, A. D.; Teixeira-Dias, J. J. C.; Goncalves, I. S. *Organometallics* **2005**, *24*, 5673–5677.
- (9) Nijhuis, C. A.; Ravoo, B. J.; Huskens, J.; Reinhoudt, D. N. *Coord. Chem. Rev.* **2007**, *251*, 1761–1780.
- (10) Dorokhin, D.; Hsu, S. H.; Tomczak, N.; Reinhoudt, D. N.; Huskens, J.; Velders, A. H.; Vancso, G. J. *ACS Nano* **2010**, *4*, 137–142.
- (11) Young, J. F.; Nguyen, H. D.; Yang, L. T.; Huskens, J.; Jonkheijm, P.; Brunsveld, L. *ChemBioChem* **2010**, *11*, 180–183.
- (12) Khashab, N. M.; Trabolssi, A.; Lau, Y. A.; Ambrogio, M. W.; Friedman, D. C.; Khatib, H. A.; Zink, J. I.; Stoddart, J. F. *Eur. J. Org. Chem.* **2009**, 1669–1673.
- (13) Wang, Z. P.; Feng, Z. Q.; Gao, C. Y. *Chem. Mater.* **2008**, *20*, 4194–4199.
- (14) Cheng, Z. Y.; Liu, S. H.; Beines, P. W.; Ding, N.; Jakubowicz, P.; Knoll, W. *Chem. Mater.* **2008**, *20*, 7215–7219.
- (15) Dubacheva, G. V.; Van Der Heyden, A.; Dumy, P.; Kaftan, O.; Auzély-Velty, R.; Coche-Guerente, L.; Labbé, P. *Langmuir* **2010**, *26*, 13976–13986.
- (16) Yan, Q.; Yuan, J. Y.; Cai, Z. N.; Xin, Y.; Kang, Y.; Yin, Y. W. *J. Am. Chem. Soc.* **2010**, *132*, 9268–9270.
- (17) Li, Q. H.; Chen, X.; Wang, X. D.; Zhao, Y. R.; Ma, F. M. *J. Phys. Chem. B* **2010**, *114*, 10384–10390.
- (18) Tomatsu, I.; Hashidume, A.; Harada, A. *Macromol. Rapid Commun.* **2006**, *27*, 238–241.
- (19) Liao, X. J.; Chen, G. S.; Liu, X. X.; Chen, W. X.; Chen, F.; Jiang, M. *Angew. Chem., Int. Ed.* **2010**, *49*, 4409–4413.
- (20) Guo, M. Y.; Jiang, M.; Pispas, S.; Yu, W.; Zhou, C. X. *Macromolecules* **2008**, *41*, 9744–9749.
- (21) Liu, J. H.; Chen, G. S.; Guo, M. Y.; Jiang, M. *Macromolecules* **2010**, *43*, 8086–8093.
- (22) Zhou, N. C.; Zhang, Z. B.; Zhu, J.; Cheng, Z. P.; Zhu, X. L. *Macromolecules* **2009**, *42*, 3898–3905.
- (23) Zhang, Z. Q.; Yuan, Y.; Sun, P.; Su, B.; Guo, J. D.; Shao, Y. H.; Girault, H. H. *J. Phys. Chem. B* **2002**, *106*, 6713–6717.
- (24) Isnin, R.; Salam, C.; Kaifer, A. E. *J. Org. Chem.* **1991**, *56*, 35–41.
- (25) Lai, J. T.; Filla, D.; Shea, R. *Macromolecules* **2002**, *35*, 6754–6756.